Effect of Al_2O_3 Concentration on Density and Structure of (CaO-SiO_2)-xAl_2O_3 Slag

RAMARAGHAVULU RAJAVARAM, HYELIM KIM, CHI-HOON LEE, WON-SEUNG CHO, CHI-HWAN LEE, and JOONHO LEE

The effect of Al_2O_3 concentration on the density and structure of CaO-SiO_2-Al_2O_3 slag was investigated at multiple Al_2O_3 mole percentages and at a fixed CaO/SiO_2 ratio of 1. The experiments were conducted in the temperature range of 2154 K to 2423 K (1881 °C to 2150 °C) using the aerodynamic levitation technique. In order to understand the relationship between density and structure, structural analysis of the silicate melts was carried out using Raman spectroscopy. The density of each slag sample investigated in this study decreased linearly with increasing temperature. When the Al_2O_3 content was less than 15 mole pct, density decreased with increasing Al_2O_3 content due to the coupling of Si (Al), whereas above 20 mole pct density of the slag increased due to the role of Al^{3+} ion as a network modifier.

DOI: 10.1007/s11663-017-0964-2

I. INTRODUCTION

CaO-SiO_2-Al_2O_3 is one of the important silicate melts in the iron- and steel-making processes. Thermo-physical properties of the slag such as density, viscosity, surface tension, and thermal conductivity are crucially important to optimize the high temperature processes. Notably, these properties are highly dependent on the silicate structure.[1] Therefore, advanced knowledge of structural information is essential to develop a thorough comprehension of the slag system.

In the CaO-SiO_2-Al_2O_3 slag system, CaO is a basic oxide that acts as a modifier in silicate melts, *i.e.*, it depolymerizes the silicate structure and provides non-bridging oxygen (NBO). The structural units of silicate melts are monomer (SiO_4^{4-}), dimer ($Si_2O_7^{6-}$), chain (SiO_3^{2-}), sheet ($Si_2O_5^{2-}$), and fully polymerized structures (SiO_2).[2] These structural units are denoted by Q^0, Q^1, Q^2, Q^3, and Q^4, respectively (Q^n notation indicates n bridging oxygens per tetrahedron). Mysen *et al.* suggested that these structural units are equilibrated according to the quantity of non-bridging oxygen atoms per cation (NBO/T).[3,4]

$$Q^1 = Q^0 + Q^2 \text{ (for NBO/T } = 2.1-4.0) \quad [1]$$

$$Q^2 = Q^0 + Q^3 \text{ (for NBO/T } = 1.0-2.1) \quad [2]$$

$$Q^3 = Q^2 + Q^4 \text{ (for NBO/T } = 0.1-1.0) \quad [3]$$

In this study, NBO/T is estimated according to Eq. [4].[5,6]

$$\frac{\text{NBO}}{\text{T}} = \frac{2X_{\text{CaO}} - 4X_{\text{Al}_2\text{O}_3}}{X_{\text{SiO}_2} + 2X_{\text{Al}_2\text{O}_3}} \quad [4]$$

On the other hand, Al_2O_3 is an amphoteric oxide whose equilibrium forms are suggested by Eqs. [5] through [7].[2]

$$Al_2O_3 = 2Al^{3+} + 3O^{2-} \quad [5]$$

$$Al_2O_3 + 5O^{2-} = 2AlO_4^{5-} \quad [6]$$

$$Al^{3+} + 4O^{2-} = AlO_4^{5-}. \quad [7]$$

In a silicate system, alumina forms Al^{3+} ions that balance the free oxygen ions and also combine with free oxygen ions to form AlO_4^{5-} ions. Accordingly, the relation between Al^{3+} and AlO_4^{5-} ions will depend on the slag basicity (or the activity of oxygen ions); Al^{3+} is more stable in the acidic region, whereas AlO_4^{5-} in the basic region.[2] If the metal cation Ca^{2+} balances the local charge, Al^{3+} may fit into the tetrahedral sites of the silicate structure. Accordingly, Si(Al) coupling occurs upon substitution of Si by Al in the tetrahedral structure of the silicate melt.[3,7–9] If there are insufficient metal cations, Al^{3+} may dissociate from the tetrahedral sites and act as a network modifier.

This structural modification may yield changes in the thermo-physical properties of silicate melts. For example, Grundy *et al.* reported the relationship between viscosity and structure of the CaO-SiO_2-Al_2O_3 system at

RAMARAGHAVULU RAJAVARAM, HYELIM KIM, and JOONHO LEE are with the Department of Materials Science and Engineering, Korea University, Anam-ro 145, Seongbuk-gu, Seoul, 02841, Republic of Korea. Contact e-mail: joonholee@korea.ac.kr CHI-HOON LEE, WON-SEUNG CHO, and CHI-HWAN LEE are with the Department of Materials Science and Engineering, Inha University, Inharo 100, Nam-gu, Incheon, 22212, Republic of Korea.
Manuscript submitted September 29, 2016.
Article published online March 16, 2017.

1773 K (1500 °C).[10] They investigated the variation of viscosity with respect to the (wt pct Al_2O_3)/[(wt pct Al_2O_3) + (wt pct CaO)] at constant SiO_2 concentrations (40, 50, 60, and 70 wt pct). The viscosity exhibited maximum values when this ratio equaled to 0.7 to 0.8, regardless the SiO_2 content. They asserted that the transition of the composition dependence in the viscosity was due to the amphoteric structure modification by Al_2O_3. Kang and Morita measured the thermal conductivity of the CaO-SiO_2-Al_2O_3 system at 1773 K and 1873 K (1500 °C and 1600 °C) at fixed CaO/SiO_2 ratios of 0.4 and 0.9, and obtained maximum thermal conductivity values when the Al_2O_3 content was at around 15 wt pct.[11] From nuclear magnetic resonance (NMR) analysis, they confirmed that AlO_4^{5-} was dominant when the Al_2O_3 content was below 15 wt pct, while Al^{3+} was high when Al_2O_3 content was above 15 wt pct.

Although density provides direct information about the silicate structure and allows observation of the amphoteric behavior of Al_2O_3, it has not been examined in conjunction with structural analysis. In this study, the relationship between density and structure of the CaO-SiO_2-Al_2O_3 slag system is investigated as a

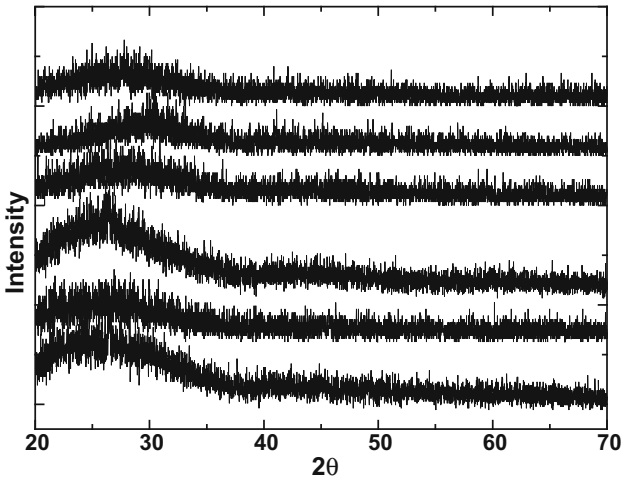

Fig. 1—The confirmation of sample vitrescence using XRD from 20 to 70 deg for CaO-SiO_2-Al_2O_3 system.

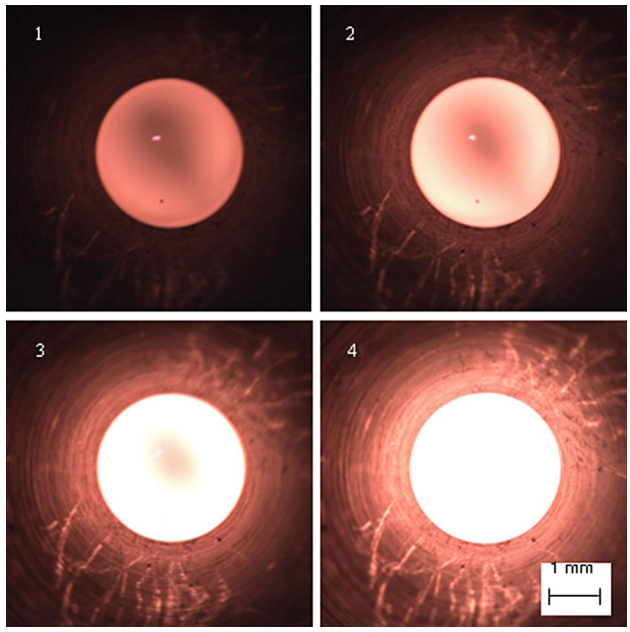

Fig. 3—Typical sample images of a slag drop in the aerodynamic levitation facility ((**1**) 1773 K (1500 °C), (**2**) 1873 K (1600 °C), (**3**) 1973 K (1700 °C), and (**4**) 2073 K (1800 °C)).

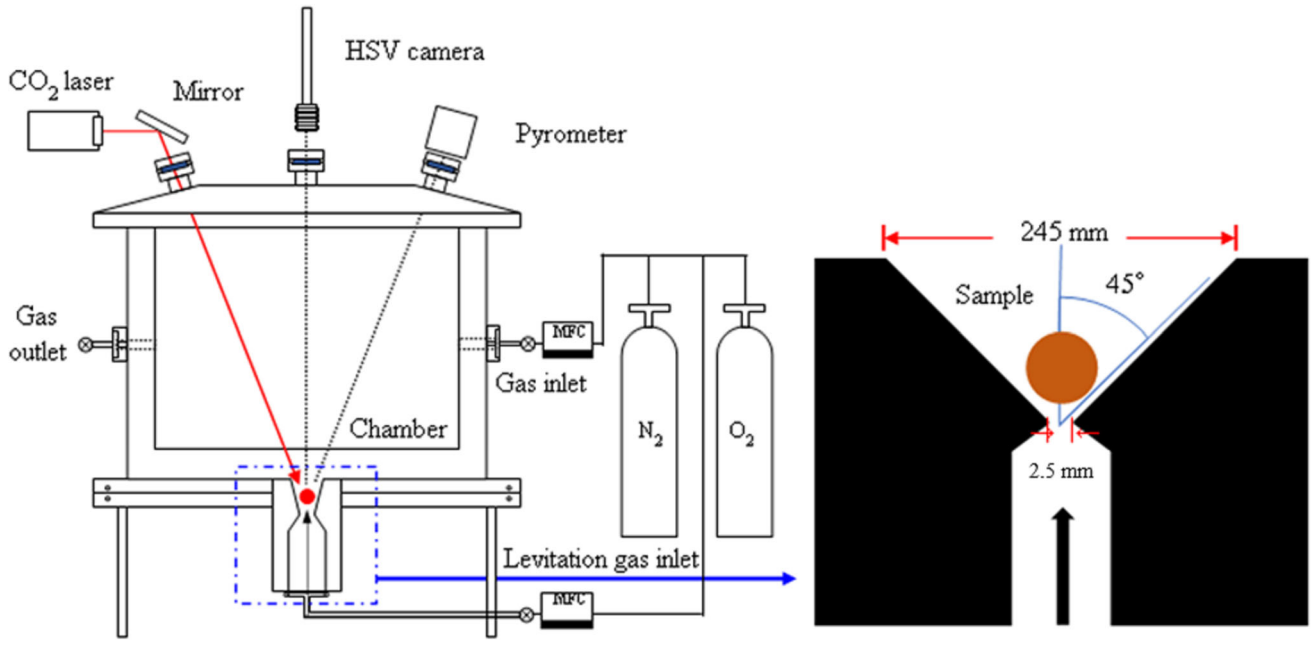

Fig. 2—Schematic illustration of the aerodynamic levitation facility.

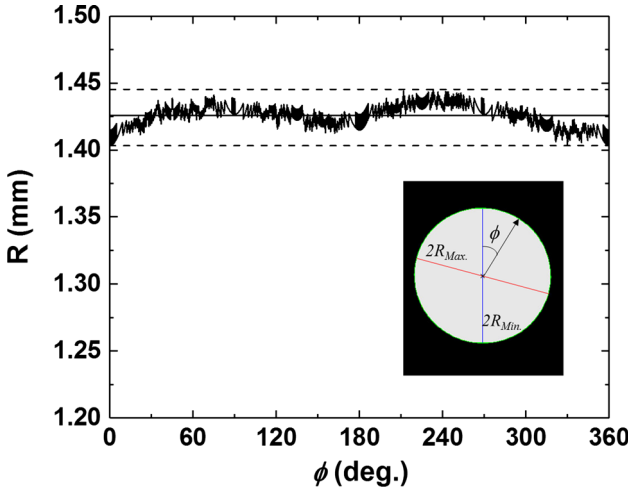

Fig. 4—Radius of a typical sample as a function of the rotation angle.

function of Al_2O_3 content at a constant ratio of $CaO/SiO_2 = 1$.

II. EXPERIMENTAL

A. *Sample Preparation*

For density measurements, six samples were prepared. The composition ranged from 4 to 24 mole pct of Al_2O_3 at a fixed CaO/SiO_2 ratio of 1. After weighing and mixing chemicals, the slag sample was pre-melted in a platinum crucible at 1853 K (1580 °C), which was above the liquidus temperature of the sample. In this study, CaO was prepared in advance by the calcination of $CaCO_3$ at 1373 K (1100 °C) for two hours in a furnace under air atmosphere. Pre-melting was performed twice in a vertical electric resistance furnace, and each time the sample was ground to fine powder to ensure homogeneity. Finally, the sample was charged in a platinum crucible and placed in the furnace for an additional 2 hours to remove internal bubbles. The vitrescence nature of the prepared samples was confirmed by X-ray diffraction (D/Max-2500V/PC, Rigaku) as shown in Figure 1. The sample composition was analyzed using scanning electron microscopy (S-4300, Hitachi) equipped with energy dispersive X-ray spectroscopy (6853-H, Horiba).

B. *Aerodynamic Levitation Method*

The aerodynamic levitation facility was used for the density measurements.[12] With this technique, the temperature range of the measurements can be higher compared to the conventional Archimedean method.[13] Figure 2 shows a schematic illustration of the experimental facility. Once a sample weighing 35 to 50 mg was placed in the sample holder, the sample was heated rapidly with a CO_2 laser (100 W, Firestar-t series, Synrad Inc., USA) with blowing O_2 gas through a conical nozzle (2.5 mm diameter) at a flow rate of 400 ml/min STP. Temperature was controlled in the range of 2154 K to 2423 K (1881 °C to 2150 °C), which was measured with a pyrometer (IR-SAS2SN, Chino, Japan). The temperature calibration was carried out by measuring the melting point of the $CaO-SiO_2$ compound. It was assumed that the emissivity of the slag was the same as that of the $CaO-SiO_2$ slag at the melting point and did not change with temperature and composition.

During the experiments, the sample images were captured with a high-speed video camera (FASTCAM MC2, Photron, Japan). Figure 3 shows typical images of the sample. The surface contour of the sample image and the corresponding diameter and volume were determined using lab-made MATLAB software. Figure 4 shows the radius of a typical sample as a function of the rotation angle ϕ. Differences between the average radius and the maximum and the minimum radii are 1.37 and 1.58 pct, respectively. If it is assumed that the vertical radius has a value between the maximum and the minimum, the maximum error in volume would be −1.80 to +1.15 pct.

C. *Raman Spectroscopy Analysis*

The structure of the silicate melts was investigated using Raman spectroscopy. For the structural analysis, two additional samples were examined together (1.87 and 32.79 wt pct Al_2O_3). The Raman spectra were recorded with a Horiba Jobin-Yvon LabRam Aramis spectrometer. A 514.5 nm beam from an Ar-ion laser was used as the excitation source. The Raman scattered light signal was collected in a backscattering geometry using a 50x microscope objective lens. The Raman excitation beam spot size was ~1 μm in diameter.

III. RESULTS

A. *Density*

Density of each slag sample is plotted as a function of temperature in Figure 5. A linear temperature dependence of density was observed: the density decreased with increasing temperature. For comparison, density values obtained from the Archimedean method are plotted with the experimental results.[13,14] The extrapolated value from the present results of the sample containing 4.23 mole pct of Al_2O_3 is slightly higher than that reported in reference 13 (the difference being ~3.7

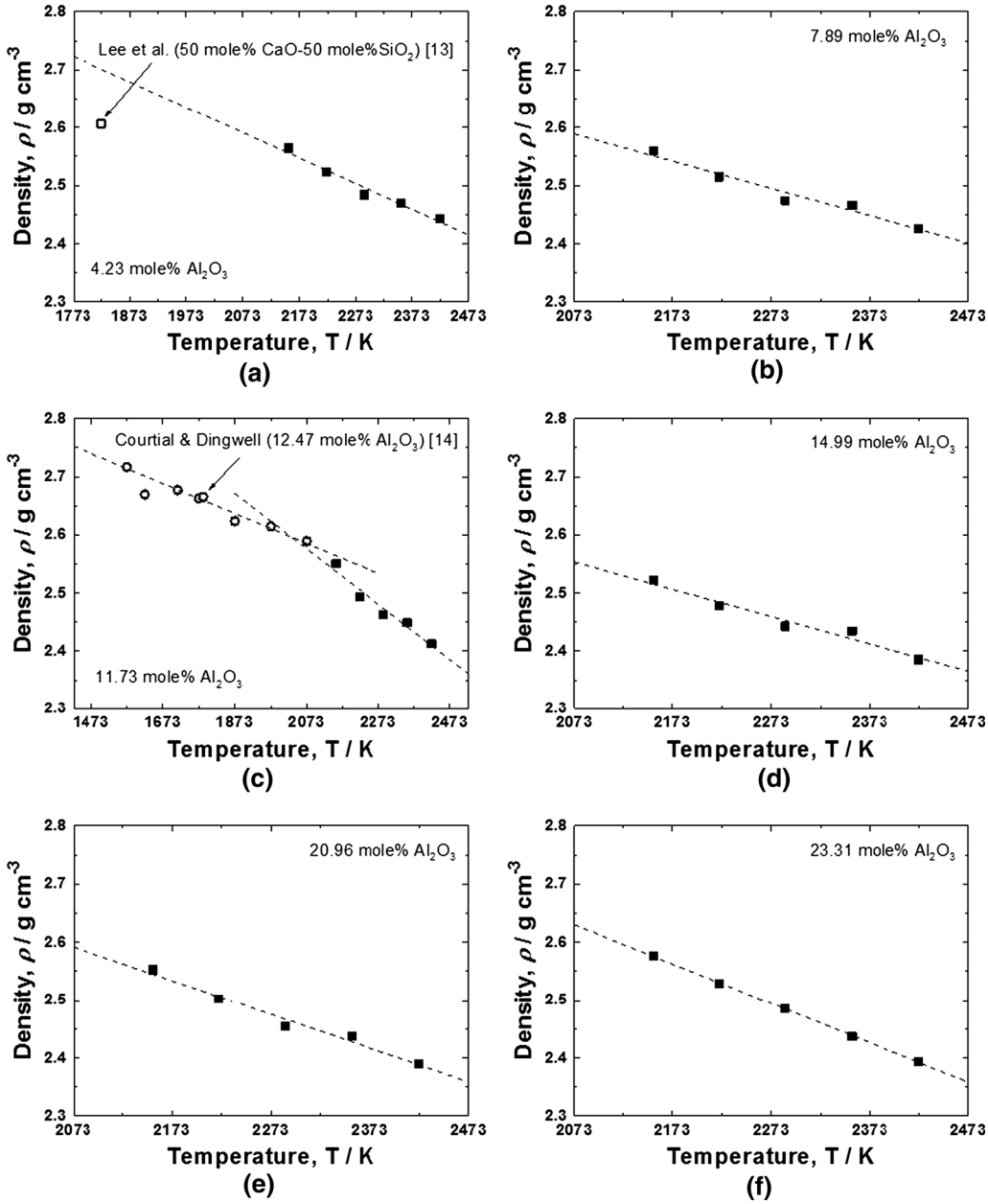

Fig. 5—Temperature dependence of density of the $CaO\text{-}SiO_2\text{-}Al_2O_3$ slags: (*a*) 4.23 mole pct Al_2O_3, (*b*) 7.89 mole pct Al_2O_3, (*c*) 11.73 mole pct Al_2O_3, (*d*) 14.99 mole pct Al_2O_3, (*e*) 20.96 mole pct Al_2O_3, and (*f*) 23.31 mole pct Al_2O_3.

pct). The results of the sample containing 11.73 mole pct Al_2O_3 show a much steeper temperature dependence than the reported data in Reference 14. They have almost the same value at 2073 K. With the Archimedean method, inaccurate data for thermal expansion of the bob might cause experimental errors. On the other hand, with the aerodynamic levitation method, the assumption of a constant emissivity might cause experimental errors. In Figure 6, the slag density is plotted with respect to mole pct of Al_2O_3. Regardless of experimental temperature, the density initially decreased with increasing Al_2O_3 content up to 15 pct, and then increased from 20

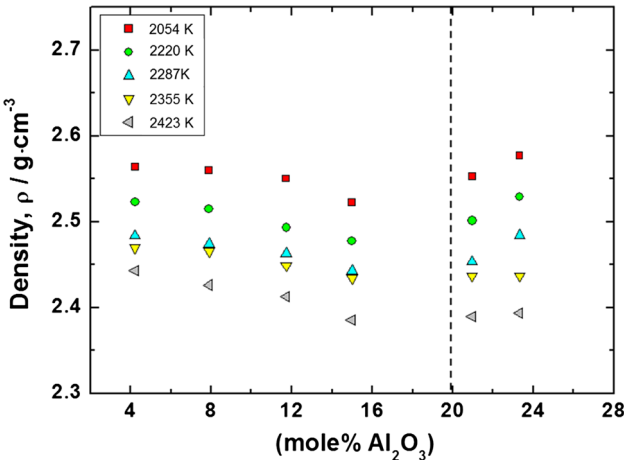

Fig. 6—The effect of concentration of Al_2O_3 on the density of silicate melts.

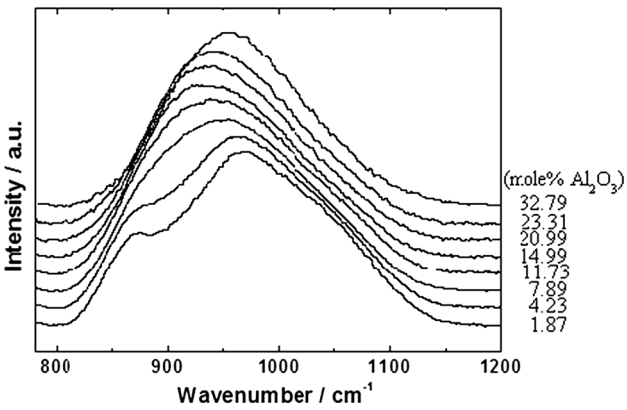

Fig. 7—Raman spectroscopy analysis of $CaO\text{-}SiO_2\text{-}Al_2O_3$ slags.

pct. The transition composition region is close to that observed in thermal conductivity measurements by Kang and Morita.[11]

B. *Raman Spectra*

Figure 7 shows the Raman spectra of the $CaO\text{-}SiO_2\text{-}Al_2O_3$ ($CaO/SiO_2 = 1$) slag samples at multiple Al_2O_3 mole percentages. In the spectra, two broad peaks appeared in the spectral range of 800 to 1200 cm^{-1} when the Al_2O_3 concentration was less than ~5 mole pct. When the Al_2O_3 content was higher than ~5 mole pct, one broad peak was observed. The maximum intensity peak position gradually shifted to the lower frequency side as Al_2O_3 concentration increased. However, at Al_2O_3 concentrations above ~15 mole pct, the peak position shifted to the higher frequency side. This transition range coincides with the results from density measurements. For a better understanding of the structural modification, deconvolution of the Raman spectra is necessary. The deconvolution of the Raman spectra was carried out using the Peakfit program (Figure 8). The peak deconvolution provided Q^0, Q^2, BO, and Q^3 units for Al_2O_3 mole percentages between 1.87 and 7.89. On the other hand, above 11.73 mole pct Al_2O_3, peak deconvolution showed the Q^2, BO, Q^3, and Q^4 units.

IV. DISCUSSION

Figure 9 shows the Raman bands frequency evolution of the silicate structure units in the samples. When Al_2O_3 content was less than 15 pct, all frequencies except that for Q^0, decreased with increasing Al_2O_3 content. As addressed before, this may be the result of the Si(Al) coupling due to the incorporation of Al-O^0 units into Si-O^0 units. On the other hand, no significant change in frequency was observed at concentrations above 20 pct. This may be the result of no additional Si(Al) coupling due to the depletion of Ca cations.

The relative areas of deconvoluted peaks correspond to the ratios of the individual silicate structure units.[15,16] In Figure 10, ratios of each structure are presented with respect to Al_2O_3 concentration. Below 15 pct Al_2O_3, the amount of Q^0 and Q^2 decreased with increasing Al_2O_3 content, while the amount of BO, Q^3, and Q^4 increased. Therefore, it is determined that Si(Al) coupling occurred and Al behaved as a network former, reinforcing the polymerization of silicate melts. On the other hand, when Al_2O_3 content was higher than 20 pct, the amount of Q^2 and Q^3 increased, while BO and Q^4 decreased as the Al_2O_3 concentration increased. The increase of Q^3 structure is much higher than that of Q^2. Considering the equilibrium of the silicate structure was determined according to Eq. [3], depolymerization of Q^4 mostly resulted in Q^3 structure enhancement. Consequently, dissociated Al^{3+} ions acted as network modifiers due to the lack of charge-balancing cations.

Liu *et al.* investigated the local atomic structure of the $CaO\text{-}SiO_2\text{-}Al_2O_3$ system ($CaO/SiO_2 = 1$ at various Al_2O_3 mole percentages) by using the neutron diffraction experiments coupled with density functional theory.[17] This study found that regardless Al_2O_3 content, Si cations were tetrahedrally coordinated. However, the coordination number of Al cations was 4 or 5. The predominant form of Al cations was AlO_4 (~70 pct), while AlO_5 was ~30 pct. The amount of AlO_5 slightly increased with increasing Al_2O_3 content to 40 pct, while that of AlO_4 slightly decreased. The results obtained by Liu *et al.* coincide with the present results that the addition of Al_2O_3 first enhances the silicate network structure with the charge compensation effect. Consequently, when the Al_2O_3 content is less than 15 pct, the density decreased with increasing Al_2O_3 content because

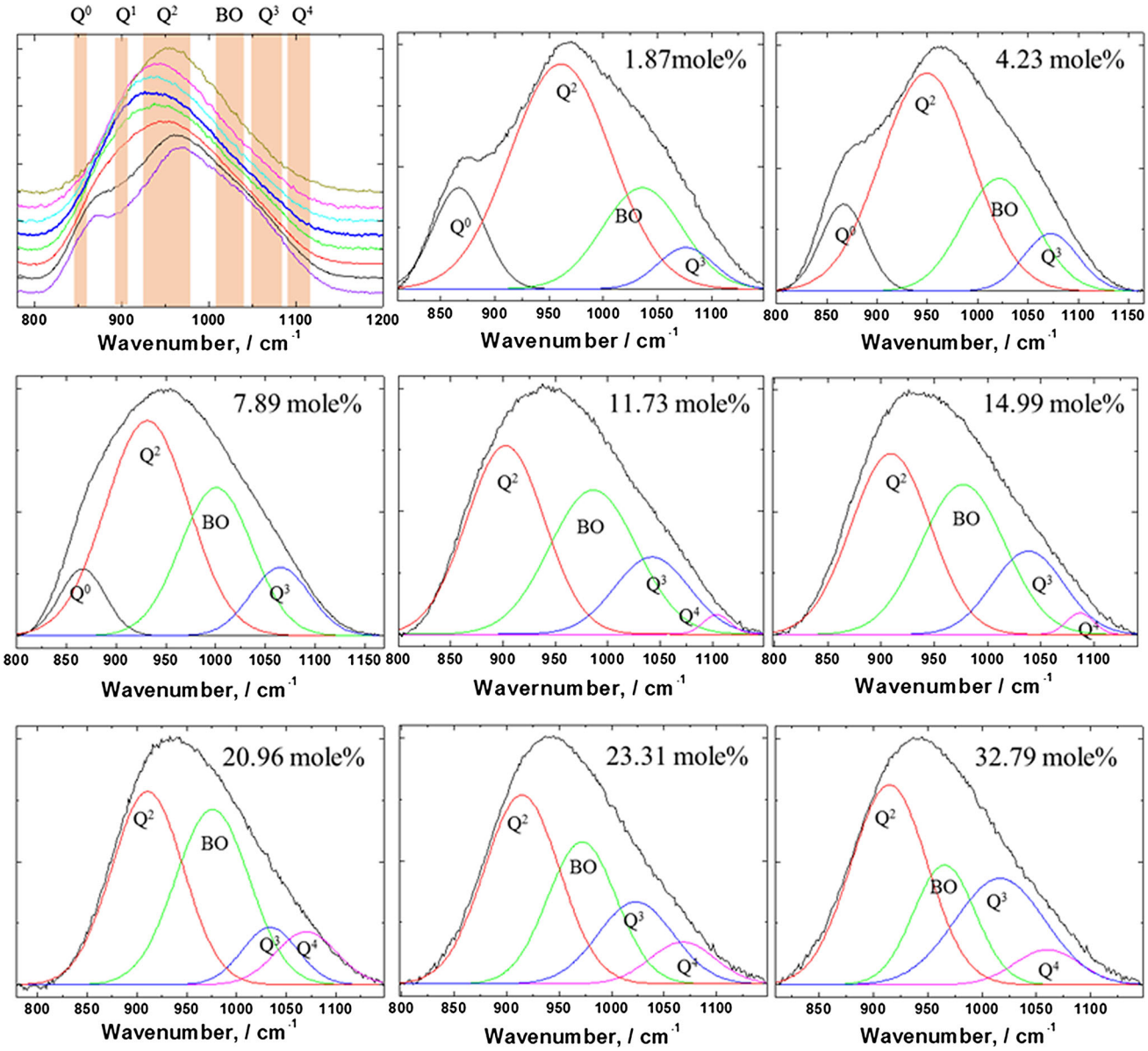

Fig. 8—The peak deconvolution of Raman spectroscopy for the slags.

the bond length of Al-O (~0.177 nm) is higher than that of Si-O (~0.160 nm).[18] However, when the Al_2O_3 content is higher than 20 pct, with the depletion of Ca cations, Al cations are surrounded by non-bridging oxygen ions, yielding the AlO_5 structure. Takehashi *et al*. reported that the formation of AlO_5 was related to the increased ionic packing factor.[19] In this composition range, therefore, density of the slag would increase with increasing the Al_2O_3 content. This behavior was confirmed in the present density measurements.

V. CONCLUSIONS

The effect of the Al_2O_3 content on the density of CaO-SiO_2-Al_2O_3 slag was investigated at a fixed CaO/SiO_2 ratio of 1 using the aerodynamic levitation method. The slag density decreased as the Al_2O_3 content increased to 15 mole pct, while the density increased at concentrations greater than 20 mole pct. The structural analysis of the slag was carried out with Raman spectroscopy. When the composition of Al_2O_3 was less than 15 mole pct, Si(Al) coupling dominantly occurred,

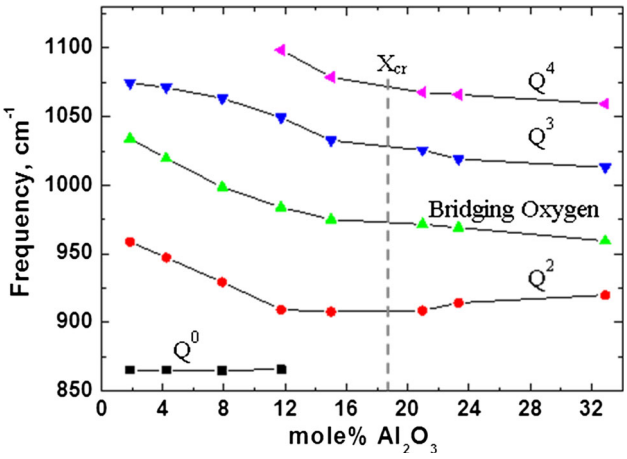

Fig. 9—The evolution of the frequencies of the bands for the CaO-SiO_2-Al_2O_3 slags.

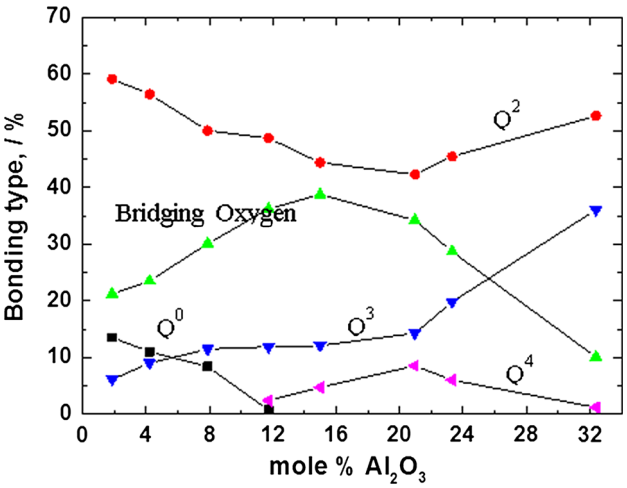

Fig. 10—The ratio of structural units of the CaO-SiO_2-Al_2O_3 slags.

resulting in increased Al-O bond length. As a result, the slag density decreased with increasing Al_2O_3 concentration. When the composition of Al_2O_3 is greater than 20 mole pct, Al^{3+} was destabilized and became a network modifier, causing the formation of the AlO_5 structure and enhancing the ionic packing factor. As a result, the slag density increased with increasing Al_2O_3 concentration.

ACKNOWLEDGMENTS

This work was supported by the Industrial Strategic technology development program (10063488, Development of earthquake resisting reinforced concrete using grade 700 MPa reinforcing bars for enhancement of seismic safety) funded by the Ministry of Trade, Industry & Energy (MI, Korea), and by the National Research Foundation of Korea (NRF) grant funded by the Korean government (MSIP) (No. NRF-2014R1A2A2A01007011). One of the authors (RR) was supported by the Korea University Grant. The authors are grateful to valuable comments from Prof. Joo-Hyun Park, Hanyang University on structure analysis with Raman spectroscopy.

REFERENCES

1. K. Mills: *ISIJ Int*., 1993, vol. 33, pp. 148–55.
2. N. Sano, W.K. Lu, P.V. Riboud, and M. Maeda: *Advanced Physical Chemistry for Process Metallurgy*, Academic Press, San Diego, 1997, p. 48.
3. B.O. Mysen, D. Virgo, and I. Kushiro: *Am. Min*., 1981, vol. 66, pp. 678–701.
4. B.O. Mysen, R.J. Ryerson, and D. Virgo: *Am. Min*., 1980, vol. 65, pp. 690–710.
5. K. Mills: *Slag Atlas*, 2nd ed., Verlag Stahleisen GmbH, Dusseldorf, 1995, p. 6.
6. B.O. Mysen and P. Richet: *Silicate Glasses and Melts-Properties and Structure*, Elsevier, Amsterdam, 2005, pp. 108–09.
7. D. Virgo, F. Seifert, and B.O. Mysen: *Carnegie Inst. Wash. Yearb*., 1979, vol. 78, pp. 506–11.
8. S.A. Brawer and W.B. White: *J. Non Cryst. Solids*, 1977, vol. 23, pp. 261–78.
9. B.O. Mysen, A. Lucier, and G.D. Cody: *Am. Min*., 2003, vol. 88, pp. 1668–78.
10. A.N. Grundy, I. Jung, A.D. Pelton, and S.A. Decterov: *Int. J. Mat. Res*., 2008, vol. 99, pp. 1195–1209.
11. Y. Kang and K. Morita: *ISIJ Int*., 2006, vol. 46, pp. 420–26.
12. K.J. Lee, M.S.V. Kumar, S.K. Jung, C.H. Lee, C.H. Lee, S. Yoda, and W.S. Cho: *J. Ceram. Process. Res*., 2012, vol. 13, pp. 476–79.
13. J. Lee, L.T. Hoai, J. Choe, and J. Park: *ISIJ Int*., 2012, vol. 52, pp. 2145–48.
14. P. Courtial and D.B. Dingwell: *Geo. Acta*., 1995, vol. 59, pp. 3685–95.
15. J.H. Park: *Metall. Mater. Trans. B*, 2013, vol. 44B, pp. 938–47.
16. J.H. Park: *Met. Mater. Int*., 2013, vol. 19, pp. 577–84.
17. M. Liu, A. Jacob, C. Schmetterer, P.J. Masset, L. Hennet, H.E. Fischer, J. Kozalily, S.S. Jahn, and A.G. Weale: *J. Phys*., 2016, vol. 28, p. 135102.
18. D.R. Lide: *CRC Handbook of Chemistry and Physics*, 86th ed., Taylor & Francis, Boca Raton, 2005, pp. 9–54.
19. S. Takahashi, D. Neuville, and H. Takebe: *J. Non Cryst. Solids*, 2015, vol. 411, pp. 5–12.